corrected Proof

Journal of
Water & Climate Change

Journal of Water and Climate Change Vol 00 No 0, 1 doi: 10.2166/wcc.2024.461

Probabilistic projections of temperature and rainfall for climate risk assessment in Vietnam

Quan Tran-Anh [a] and Thanh Ngo-Duc [b,*]

[a] Faculty of Environment, Hanoi University of Mining and Geology, Hanoi, Vietnam
[b] Department of Space and Applications, University of Science and Technology of Hanoi (USTH), Vietnam Academy of Science and Technology (VAST), Hanoi, Vietnam
*Corresponding author. E-mail: ngo-duc.thanh@usth.edu.vn

QT-A, 0000-0003-1201-0161; TN-D, 0000-0003-1444-7498

ABSTRACT

In this study, we developed a probabilistic model using the surrogate mixed model ensemble (SMME) method to project temperature and rainfall in Vietnam under the Representative Concentration Pathway (RCP) 4.5 and 8.5 scenarios. The SMME model combines patterns from 31 global climate models participating in the Coupled Model Intercomparison Project Phase 5 (CMIP5) and their weighted model surrogates. Testing for the period of 2006–2018 demonstrated the SMME's ability to encompass observed temperature and rainfall changes. By the end of the 21st century, there is a 5% probability of average temperature increase exceeding 6.29 °C, and a 95% probability of minimum temperature increasing by more than 2.21 °C during 2080–2099 under RCP8.5 compared to 1986–2005. Meanwhile, rainfall is projected to slightly increase, with an average rise of 6.12% at the 5% probability level. The study also quantified the contributions of uncertainty sources – unforced, forced, and scenario-related – to the projection results, revealing that unforced uncertainty dominates the total signal at the beginning of the 21st century and gradually decreases, while forced uncertainty remains relatively moderate but increases gradually over time. As we approach the end of the century, scenario uncertainty dominates, accounting for 75–80% of the total signal.

Key words: climate extreme, CMIP5, probabilistic projection, surrogate mixed model ensemble, Vietnam

HIGHLIGHTS

- A probabilistic dataset of daily temperature and rainfall in Vietnam has been constructed, providing valuable insights into future changes in Vietnam.
- The dataset is accessible online at no cost.
- The contributions of three sources of uncertainty, namely, unforced uncertainty, forced uncertainty, and scenario uncertainty to the projection results in Vietnam have been quantified.

GRAPHICAL ABSTRACT

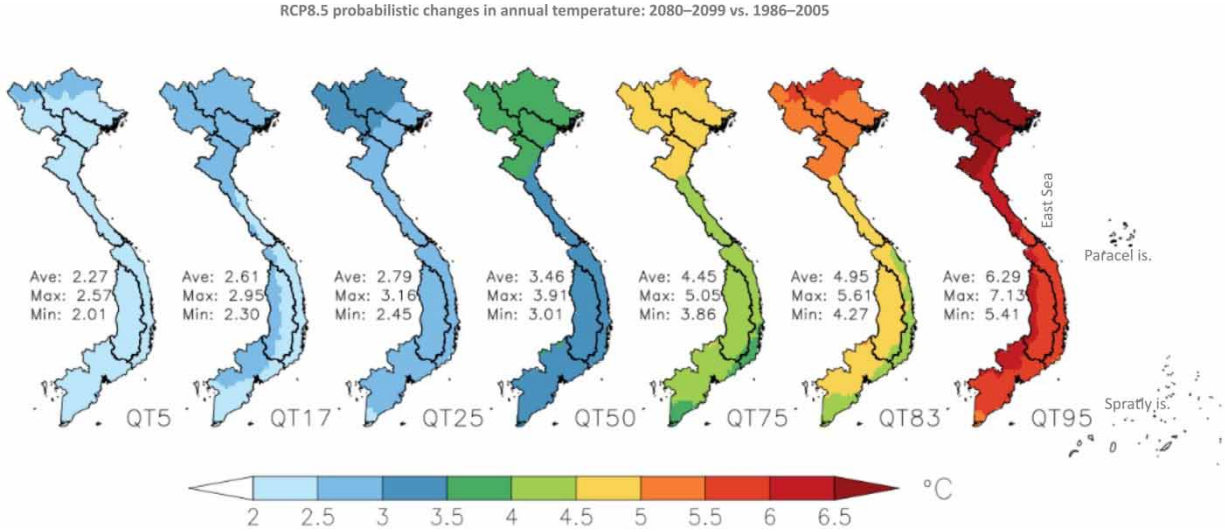

INTRODUCTION

Climate change is a global phenomenon with widespread impacts, posing significant challenges to our planet nowadays (Arias *et al.* 2021). To cope with climate change, it is important to possess reliable future climate projections, typically derived from outputs of global climate models (GCMs). Both studies on the impacts of climate change and response policies heavily rely on information about potential climate extremes (Seneviratne *et al.* 2012; Supari *et al.* 2020). Nevertheless, it has been demonstrated that GCMs often underestimate extreme values (Kitoh & Endo 2016; Iles *et al.* 2020; Nishant *et al.* 2022). Furthermore, climate change assessments often employ projections directly from a set of GCMs, such as those utilized in the Fifth Phase of the Coupled Model Intercomparison Project (CMIP5; Taylor *et al.* 2012), or from their downscaling products, as practiced within the Coordinated Regional Climate Downscaling Experiment-Southeast Asia (CORDEX-SEA) framework (Tangang *et al.* 2020; Herrmann *et al.* 2022). These sets of model outputs typically involve a limited number of models under a constrained set of future greenhouse gas scenarios, leading to incomplete coverage of the entire range of future probabilities.

To address the aforementioned limitation, probabilistic approaches are applied (e.g., Rasmussen *et al.* 2016; Raftery *et al.* 2017; Vargas Zeppetello *et al.* 2022). Unlike relying solely on a limited set of GCM projections and specific scenarios, probabilistic methods systematically integrate models, scenarios, and related uncertainty quantifications into projection results. Thus, they can encompass all possible probabilities and consequences arising from diverse future scenarios, particularly accounting for rare yet highly impactful extreme events that are often missed by GCMs (Rasmussen *et al.* 2016). While numerous studies have focused on quantifying the probability distribution of future change on a large scale, such as the country-specific level or above (Raftery *et al.* 2017; Liu & Raftery 2021; Chen *et al.* 2023), there have also been works focusing on local changes (Schölzel & Hense 2011; Kopp & Rasmussen 2015; Rasmussen *et al.* 2016). For instance, Chen *et al.* (2023) employed pattern scaling to refine global climate change projections to local scales, enabling them to obtain projections of long-term temperature for any region of the world. However, their method has a relatively coarse resolution (2.5° × 2.5°), limiting its applicability to large areas exclusively. On the other hand, Kopp & Rasmussen (2015) used the surrogate mixed model ensemble (SMME) approach to estimate the probabilities of changes in both precipitation and temperature at the U.S. county-level, achieving a higher horizontal resolution of up to 1/8° × 1/8° (~14 km). The SMME method relies on probabilistic projections from the Model for the Assessment of Greenhouse Gas Induced Climate Change (MAGICC) (Meinshausen *et al.* 2011) of global mean temperature change to evaluate the GCM outputs. It then constructs a surrogate model (SM) to capture the extreme portion of the probability distribution that GCMs cannot identify. The SMME has been applied to quantitatively analyze economic risks posed by climate change in the United States (Houser *et al.* 2015; Kopp & Rasmussen 2015). While other techniques, such as the Bayesian Model Averaging (Tebaldi *et al.* 2005) and the Weighted Interval Combination (Luo *et al.* 2019) approaches, also combine multiple model projections, the SMME has the advantage of being able to explicitly represent uncertainty contributors by integrating both parametric perturbation

uncertainties from MAGICC and structural uncertainties through the use of SMs (Rasmussen *et al.* 2016). Thus, the SMME can provide better coverage of potential futures that could be missed by raw GCM ensembles.

With over 3,200 km of coastline and many cities located in low-lying areas, Vietnam is highly vulnerable to climate change (Dasgupta *et al.* 2007; MONRE 2020). According to the Climate Risk Index report of 2018 (David *et al.* 2018), Vietnam is among the countries most impacted by extreme events, ranking fifth in 2016 and eighth for the period 1997–2016. Climate change manifestations, such as increases in temperatures and altered precipitation patterns, significantly affect socioeconomic activities and impede growth (Espagne *et al.* 2021; World Bank 2022). The cumulative direct impact on various socioeconomic sectors in Vietnam leads to an average annual gross domestic product loss of 4.5, 6.7, and 10.8% for respective increases in global warming levels of 1.5, 2, and 3 °C relative to the pre-industrial period of 1851–1900 (Espagne *et al.* 2021).

In Vietnam, future climate projections primarily rely on downscaled GCM outputs using both statistical methods (MONRE 2009, 2012; Tran-Anh *et al.* 2022, 2023) and dynamical approaches (MONRE 2012, 2016, 2020; Ngo-Duc *et al.* 2014; Katzfey *et al.* 2016; Trinh-Tuan *et al.* 2019; Nguyen-Duy *et al.* 2023). However, it is important to note that these studies were constrained by the use of only a restricted number of CMIP GCMs. For example, in the national report on climate change and sea level rise in Vietnam (MONRE 2020), only 16 dynamical downscaling experiments based on 10 CMIP5 GCMs were employed. As discussed earlier, the existing projections for Vietnam cannot cover the entire range of future probabilities, and they may particularly miss rare yet highly impactful extreme events. It is crucial to emphasize that projected information on extremes is particularly vital for adaptation planning in a country highly vulnerable to climate change like Vietnam. Therefore, in this study, we made a first attempt to provide probabilistic projections of temperature and rainfall in Vietnam using the SMME approach. The results are expected to offer valuable inputs for studies assessing climate change and its impacts on socioeconomic activities during the 21st century, supporting adaptation planning to cope with climate change in Vietnam.

DATA AND METHOD

Model and station data

To perform the probabilistic projection for Vietnam, we used outputs from 31 CMIP5 GCMs (Table 1). These outputs include daily temperatures and rainfall for the baseline period 1986–2005, and projections for the future period 2006–2099, considering Representative Concentration Pathway (RCP) 4.5 and 8.5 scenarios (Moss *et al.* 2010). We chose RCP4.5 and RCP8.5 to align with the scenarios used in the latest national report on climate change and sea level rise in Vietnam (MONRE 2020). MONRE (2020) has prioritized these two scenarios: the moderate scenario RCP4.5, considering active international efforts to mitigate climate change, and the high greenhouse gas concentration scenario RCP8.5, enabling preparation for a potential worse-case future.

The daily temperatures (daily average, daily maximum, and daily minimum) and rainfall from the aforementioned 31 GCMs have been statistically downscaled to a 10-km resolution for Vietnam using the Bias Correction Spatial Disaggregation (BCSD) technique (Tran-Anh *et al.* 2022). This downscaled dataset is referred to as CMIP5-VN. CMIP5-VN has undergone validation, and the results demonstrate its overall good performance across different sub-climatic regions of Vietnam.

The observational gridded dataset, referred to as OBS, for rainfall and temperatures was described by Tran-Anh *et al.* (2022). OBS is used to downscale the SMME results (explained below) from the average monthly scale to the daily temporal resolution. OBS has a spatial resolution of $0.1° \times 0.1°$ and covers the period 1986–2005. OBS's temperature was constructed using data from 147 stations and the Kriging interpolation method (Switzer 2014). Meanwhile, OBS's rainfall was constructed with the Spheremap method (Willmott *et al.* 1985), utilizing daily data from 481 rainfall stations across Vietnam.

For validation purposes, we randomly selected seven stations within the seven climate sub-regions of Vietnam, as identified by Nguyen & Nguyen (2004). The observed changes in temperature and rainfall data from these seven stations between the period 2006–2018 and the baseline period 1986–2005 are compared to the changes estimated by the newly constructed dataset (see the next section for details). The locations of the seven selected station are displayed in Figure 1.

Probabilistic projection method

We employed the surrogate mixed model ensemble (SMME) technique, as described by Kopp & Rasmussen (2015), to quantify the probability of temperature and rainfall changes in the 21st century in Vietnam. The SMME method utilizes probabilistic projections of global mean temperature change from the simple MAGICC (Meinshausen *et al.* 2011) to assign weights to GCM outputs. Subsequently, the SMME constructs model surrogates that capture the extreme tails of

Table 1 | The selected CMIP5 GCMs, SMs, their characteristics, bin assignments, and corresponding SMME probability weights used for the RCP4.5 scenario

SMME bin	Model	ΔT_global (°C)	MAGICC6's quantile	SMME weight
1	SM-GFDL-ESM2G	1.03	4	0.04
	SM-GISS-E2-R-CC	1.03	4	0.04
2	SM-GFDL-ESM2G	1.13	10	0.02
	SM-GISS-E2-R-CC	1.13	10	0.02
3	GFDL-ESM2G	1.17	12	0.04
	GISS-E2-R-CC	1.28	19	0.04
4	GISS-E2-R	1.32	21	0.0667
	GISS-E2-H-CC	1.49	31	0.0667
	GISS-E2-H	1.62	38	0.0667
5	BCC-CSM1-1-M	1.69	43	0.02
	MRI-CGCM3	1.7	44	0.02
	NorESM1-M	1.72	44	0.02
	CESM1-BGC	1.72	44	0.02
	MPI-ESM-LR	1.73	45	0.02
	IPSL-CM5B-LR	1.73	45	0.02
	BCC-CSM1-1	1.76	45	0.02
	CCSM4	1.83	49	0.02
	MPI-ESM-MR	1.85	50	0.02
	MIROC5	1.89	51	0.02
6	CNRM-CM5	2.06	61	0.0167
	ACCESS1-3	2.25	71	0.0167
	CMCC-CM	2.29	72	0.0167
	CMCC-CMS	2.34	74	0.0167
	IPSL-CM5A-LR	2.36	75	0.0167
	CSIRO-Mk3-6-0	2.37	75	0.0167
	BNU-ESM	2.37	75	0.0167
	ACCESS1-0	2.38	76	0.0167
	IPSL-CM5A-MR	2.4	77	0.0167
	HadGEM2-CC	2.42	78	0.0167
	CESM1-CAM5	2.45	79	0.0167
	CanESM2	2.5	80	0.0167
7	MIROC-ESM	2.57	82	0.0267
	MIROC-ESM-CHEM	2.66	85	0.0267
	HadGEM2-ES	2.74	87	0.0267
8	GFDL-CM3	2.9	89	0.02
	SM-MIROC-ESM-CHEM	2.93	90	0.02
9	SM-GFDL-CM3	3.49	96	0.03
	SM-MIROC-ESM-CHEM	3.49	96	0.03
10	SM-GFDL-CM3	4.22	99	0.01
	SM-MIROC-ESM-CHEM	4.22	99	0.01

the MAGICC probability distribution. It is important to note that these extreme tails are generally not represented by the original GCM ensemble. The key steps of the SMME method are summarized below.

Global warming projections by MAGICC

The MAGICC model (Meinshausen *et al.* 2011) is used to project global temperature changes under different greenhouse gas scenarios. Various versions of the MAGICC model have been widely employed by the climate community, with MAGICC6 specifically utilized to establish the probability distribution of global temperature increase in the Fifth Assessment Report (AR5) of the Intergovernmental Panel on Climate Change (IPCC) (Collins *et al.* 2013). For each RCP4.5 and RCP8.5 scenario (Moss *et al.* 2010), the probability distribution of global temperature increases is constructed using MAGICC6 in probabilistic

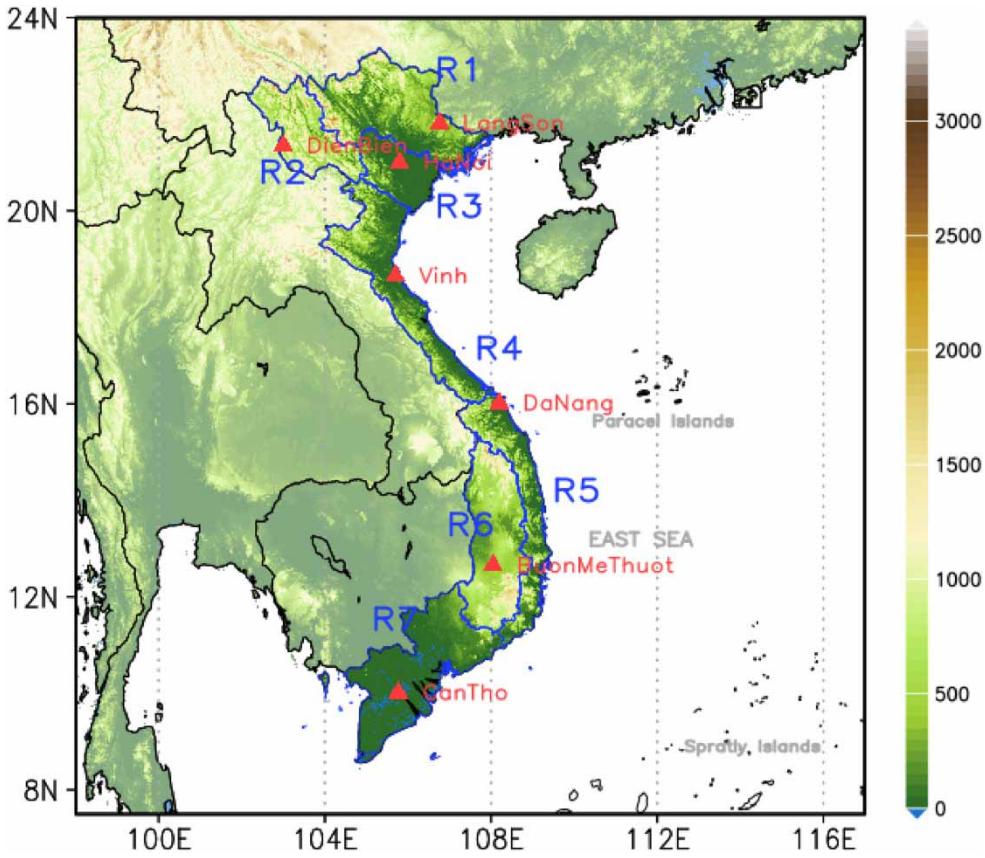

Figure 1 | Location of seven meteorological stations (red triangles) and seven climate sub-regions of Vietnam (blue lines) overlaid on a terrain altitude map (shaded, in m), extracted from the HydroSHEDS data (Lehner *et al.* 2008).

mode with 600 simulations (Meinshausen *et al.* 2011), wherein each simulation incorporates distinct input parameters. The quantile ranges of MAGICC6 are then determined based on the outputs from these 600 runs. Accordingly, the 5th, 7th, 83rd, and 90th percentiles of these 600 runs correspond to temperature increases of 1.5, 1.6, 4.9, and 5.9 °C per CO_2 doubling, respectively (Kopp & Rasmussen 2015).

Monthly SMME at global scale

When considering a projection from either a CMIP5 GCM or a MAGICC6 experiment, we denote the variable ΔT_{global} (°C) representing the change in global temperature at a future time point relative to the period 1986–2005. In addition, ΔT_{FF} represents the average ΔT_{global} for the far future period 2080–2099.

In the initial step, the ΔT_{FF} values projected by MAGICC6 are utilized to establish 10 percentile bins with unequal widths: [0,8], [8,12], [12,20], [20,40], [40,60], [60,80], [80,88], [88,92], [92,98], and [98,100]. Notably, the low and high percentile bins are defined with narrower widths to enhance the SMME model's ability to identify extreme scenarios.

Subsequently, each CMIP5 GCM model is assigned to the corresponding percentile bin based on its projected ΔT_{FF} value. It may happen that certain percentile bins from MAGICC6 lack representation by any CMIP5 model, such as the 1st, 2nd, 9th, and 10th bins in the RCP4.5 scenario, or may be represented by only one model, for example, the 8th percentile bin in the RCP4.5 scenario (Table 1). In such cases, SMs are constructed to ensure that each of these percentile bins is represented by two models in total. The CMIP5 GCMs selected to build the SM are those with ΔT_{FF} values closest to the centered ΔT_{FF} of MAGICC6 for the missing bin.

Let us consider a GCM called A, which has been selected to construct an SM named SM-A. By utilizing a linear model, we can fit the projected results of a climate variable X_A from model A, given a specific scenario s, grid cell i, and future time t as

follows:

$$X_{A,s,i}(\Delta T, t) = a_{A,s,i} \times \Delta T + b_{A,i} + \varepsilon_{A,s,i}(t) \quad (1)$$

where $a_{A,s,i}$ is the regression coefficient, $b_{A,i}$ is the average value of X_A during the baseline period, $\varepsilon_{A,s,i}$ is the error of the estimate, and ΔT denotes the change in global mean temperature relative to the baseline period 1986–2005. The term $a_{A,s,i} \times \Delta T$ is referred to as the estimated forced climate change, while $\varepsilon_{A,s,i}(t)$ represents the estimated unforced climate variability.

Then, the climate variable X_{SMA} of SM-A is given by:

$$X_{\mathrm{SMA},s,i}(\Delta T, t) = \beta \times a_{A,s,i} \times \Delta T + b_{A,i} + \varepsilon_{A,s,i}(t) \quad (2)$$

where $\beta = \Delta T_{\mathrm{MAGICC6},s,\mathrm{FF}} / \Delta T_{A,s,\mathrm{FF}}$ is a multiplicative factor reflecting the difference between the mean global temperature change in the given bin of MAGICC6 and the mean global temperature change of model A at the far future period 2080–2099.

Next, the variables of SM-A are downscaled to a 10-km resolution for the Vietnam territory using the BCSD method, which was also applied to generate the CMIP5-VN dataset (Tran-Anh *et al.* 2022). The downscaled dataset derived from these SMs is referred to as SM-VN.

Thereafter, a probability weight is assigned to each model based on two factors: the width of the percentile bin and the number of models sharing that bin (Table 1, Supplemental Table S1). Models falling within the same bin are given equal weights. For instance, in Table 1, the fourth bin corresponds to the percentile range [20, 40], which includes three models: GISS-E2-R, GISS-E2-H-CC, and GISS-E2-H. Consequently, these three models are assigned equal weights (0.0667), calculated as the width of the bin (20%) divided by the total number of models (3).

Finally, the SMME model is constructed by synthesizing the patterns of the CMIP5 GCMs and SMs using their respective probability weights. It is worth noting that only monthly values at global scale are used in the above-mentioned steps.

We observe that $\Delta T_{\mathrm{global}}$, as represented by the GCMs, only covers the 12th–89th percentiles of the MAGICC6 results (corresponding to 1.13–2.9 °C increases in global temperature at the end of the 21st century) for RCP4.5 (Table 1) and 12th–83rd percentiles (equivalent to 2.59–6.53 °C increases) for RCP8.5 (Supplemental Table S1). Meanwhile, the SMME models, which include both the CMIP5 GCMs and SMs, can encompass the entire range of $\Delta T_{\mathrm{global}}$ represented in MAGICC6 for both scenarios (Supplemental Figure S1). This demonstrates that the SMs could well capture the extreme intervals not represented by the CMIP5 GCMs, thus enhancing the coverage of future climate projections.

Daily SMME for Vietnam

The local warming probability distribution for Vietnam is derived from the global SMME results, applying the pattern scaling technique (Santer *et al.* 1990; Tebaldi & Arblaster 2014). The local changes of a variable X from either a CMIP5-VN or an SM-VN experiment can be expressed using Equation (1) where i indicates a specific 10-km resolution grid cell in Vietnam and ΔT represents the estimation based on a 30-year moving average. Subsequently, the monthly SMME projections for each 10-km grid cell in Vietnam are obtained by aggregating the results from the component CMIP5-VN and SM-VN experiments, using weights received from the respective global models.

The monthly SMME projections, once generated, are further downscaled to daily temporal resolution using the random resampling technique of the BCSD approach outlined by Wood *et al.* (2002, 2004). This temporal-downscaling process involves selecting a random year from the historical period (1986–2005 in this study) as a reference for a given future year. Then, the monthly averages of the future year are disaggregated into daily data by adjusting the daily gridded OBS dataset. Temperature adjustments are made using addition, while rainfall adjustments employ multiplication, ensuring that the monthly mean of the future data remains unchanged. The final daily dataset is referred to as SMME-VN.

The interest in producing the daily SMME-VN dataset arises from the need to quantitatively assess future climate change risks and extremes (MONRE 2020), typically represented by a set of extreme indices, using daily information. For instance, the joint World Meteorological Organization Commission on Climatology (CCl) and the Climate Variability and Prediction (CLIVAR) Expert Team on Climate Change Detection and Indices (ETCCDI) has worked to define 27 core climate indices from daily temperature and rainfall data (Karl *et al.* 1999). Given that the advantage of probabilistic projections lies in the ability to account for extreme events, daily data becomes essential, among other reasons, for subsequently estimating

associated extreme indices. These indices not only aid in quantifying future extremes but can also be used as inputs for further impact assessment studies.

We acknowledge that the BCSD approach applied in this study, along with its random resampling technique, does not maintain the daily correspondence of the coarse spatial resolution GCMs. Despite this limitation, BCSD has been extensively employed for temporal disaggregation of GCMs' projections in impact assessments worldwide (e.g., Zhang *et al.* 2017; Duan *et al.* 2021; Tran-Anh *et al.* 2022; Atiah *et al.* 2023; Michalek *et al.* 2024; Rabezanahary Tanteliniaina & Andrianarimanana 2024). Some prior studies have compared the performance of this temporal disaggregation method with traditional daily-preserving downscaling approaches (e.g., Maurer and Hidalgo 2008; Yang *et al.* 2019). For instance, Maurer and Hidalgo (2008) indicated that both methods exhibit some skill in reproducing daily variability of observed rainfall and temperature extremes, with a certain advantage for the latter approach. It is worth noting that recently developed downscaling approaches, such as the Quantile-Preserving Localized-Analog Downscaling (Gergel *et al.* 2024), allow for the efficient preservation of GCMs' daily variability. These approaches could be considered in our future studies.

Sources of uncertainty

Besides the importance of probabilistic projections for temperature and rainfall, determining the uncertainty associated with the projections' results is also crucial. Hawkins & Sutton (2009) divided the sources of the total model uncertainty (referred to as UC) into three distinct components: the forced uncertainty of the model (referred to as F, arising from variations in climate model responses to external radiative forcing, such as greenhouse gases); the intrinsic uncertainty, also known as the unforced uncertainty component (referred to as U, arising from the natural internal variability of the climate system); and the scenario uncertainty (referred to as S, arising from uncertainties in future greenhouse gas scenarios, as the exact evolution of future emission remains unknown):

$$\mathrm{UC}(t) = F(t) + U(t) + S(t) \tag{3}$$

Assuming that the scenarios have equal probabilities of occurring, the forced uncertainty of the models is estimated by calculating the weighted sum of the variances associated with the forced change of each model. Similarly, the unforced uncertainty component of the models is estimated by calculating the weighted sum of the variances associated with the unforced change of each model. The scenario uncertainty is then estimated as the absolute difference between the average values of the weighted models (N models in total) for the two scenarios RCP4.5 and RCP8.5:

$$S(t) = \left| \frac{1}{N} \left(\sum_{\mathrm{Model}} (w_M \times M)_{\mathrm{RCP8.5}} - (w_M \times M)_{\mathrm{RCP4.5}} \right) \right| \tag{4}$$

where N represents the number of models, M is the average model value, and w_M represents the weight assigned to model M for scenario s, as identified during the SMME model building step (Table 1, Supplemental Table S1).

In this study, we assume zero forced uncertainty ($F = 0$) and zero uncertainty of the scenarios ($S = 0$) at the beginning of the future period, with the unforced uncertainty representing 100% of the total model uncertainty.

RESULTS AND DISCUSSION

Performance of the SMME projections

To the best of our knowledge, although the SMME method has been applied in various studies, there has been no study to date that validates the accuracy of projected temperature and rainfall. Here, for the first time, we attempt to assess the reliability of the SMME projections over specific locations of Vietnam for the projection period 2006–2018, a timeframe for which we already have observed data. We compare the projected products with observed data obtained from seven randomly selected meteorological stations (refer to Figure 1 for the station locations). Figure 2 displays temperature anomalies during the period 2006–2018 relative to the baseline period 1986–2005 for these seven stations. There is a significant increase in average temperature during 2006–2018 compared to the baseline period. The observed data exhibit a minimum rise of 0.37 °C at the Da Nang station and a maximum increase of 0.65 °C at the Hanoi station. The SMME models well depict the range of temperature increase for both RCP4.5 and RCP8.5 scenarios during 2006–2018, effectively encompassing the

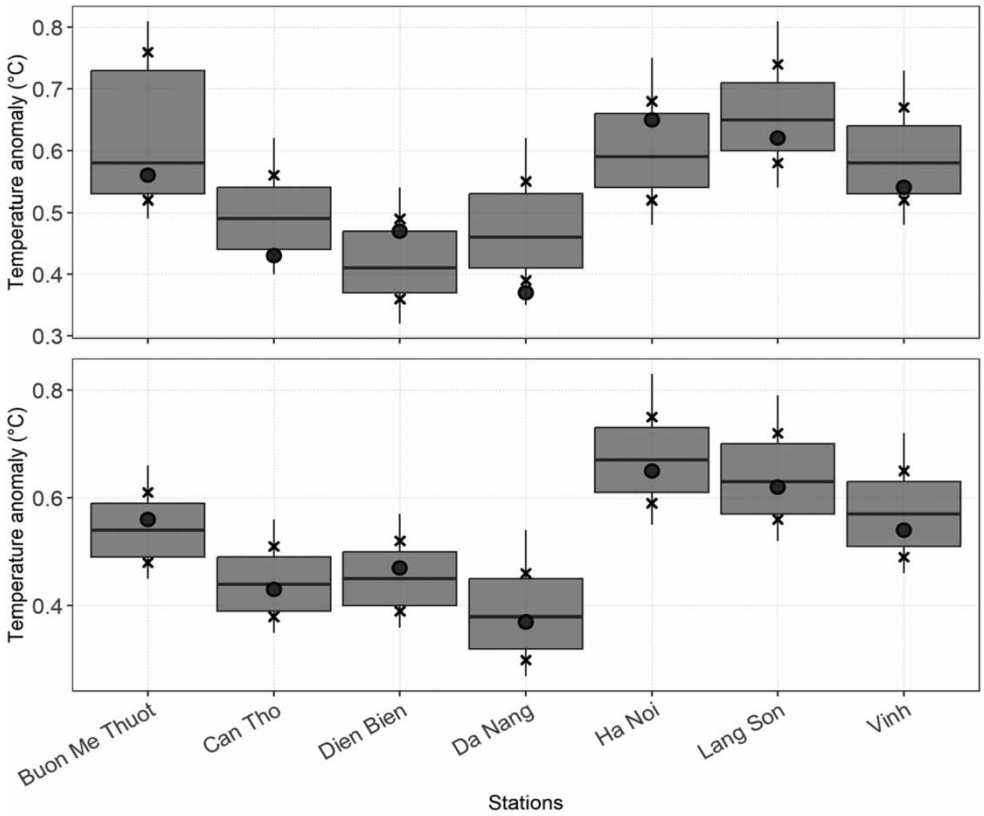

Figure 2 | Box plots of temperature anomalies projected by the SMME models at seven meteorological stations for the period 2006–2018 relative to the period 1986–2005 under RCP4.5 (top) and RCP8.5 (bottom). The lower and upper ends as well as the black horizontal line inside the box, respectively, indicate the first quartile, third quartile, and median. Cross signs denote the 17th and 83rd percentiles. The black vertical line extends to the 5th and 95th percentiles. Black dots represent the observations.

observed values at all seven stations. The observed data points are generally close to the median model within the SMME models under RCP8.5, although they can fall outside the interquartile range of the SMME models under RCP4.5 at certain stations such as Can Tho and Da Nang. In all cases, the observed data points consistently fall within the 5th to 95th percentile interval of the SMME models, which ranges from 0.21 °C (0.22°C) at Can Tho (Dien Bien) station to 0.28 °C (0.32 °C) at Hanoi (Buon Me Thuot) station under RCP4.5 (RCP8.5).

It should be noted that despite RCP8.5 representing a scenario with higher radiative forcing, its divergence from RCP4.5 becomes clear only from the mid-21st century (Collins *et al.* 2013; Xin *et al.* 2013). Previous studies indicated that projection signals over a specific area, particularly in the near future period, typically exhibit uncertainties due to various factors such as projected greenhouse gas concentrations, model imperfections, and natural variability (Sorteberg & Kvamstø 2006; Deser *et al.* 2012; de Elía *et al.* 2013). Nguyen-Thuy *et al.* (2021) estimated the time of emergence (TOE), i.e. the time that the climate change signal exceeds the above uncertainties, for projected temperature and rainfall in Vietnam under RCP4.5 and RCP8.5. They found that the TOE of annual and seasonal average temperatures generally started after 2018 for both scenarios. This implies that the selected period for comparison with observational data in our present study, 2006–2018, predates the time when the TOE could be detected for both RCPs. As a consequence, the impact of the chosen RCP on temperature changes could be indistinguishable from the impact of other factors mentioned above. This elucidates why, despite RCP8.5 depicting an extreme future scenario, its median model can still exhibit a closer proximity to the observational data points compared to RCP4.5 during the early-century period (2006–2018).

The SMME projections for rainfall anomalies during 2006–2018 are shown in Figure 3. Except for the Hanoi station under RCP4.5 and the Buon Me Thuot station under RCP8.5, the projected rainfall generally shows an increase compared to the baseline period. The changes in rainfall, according to the SMME median model (observed data), at the seven

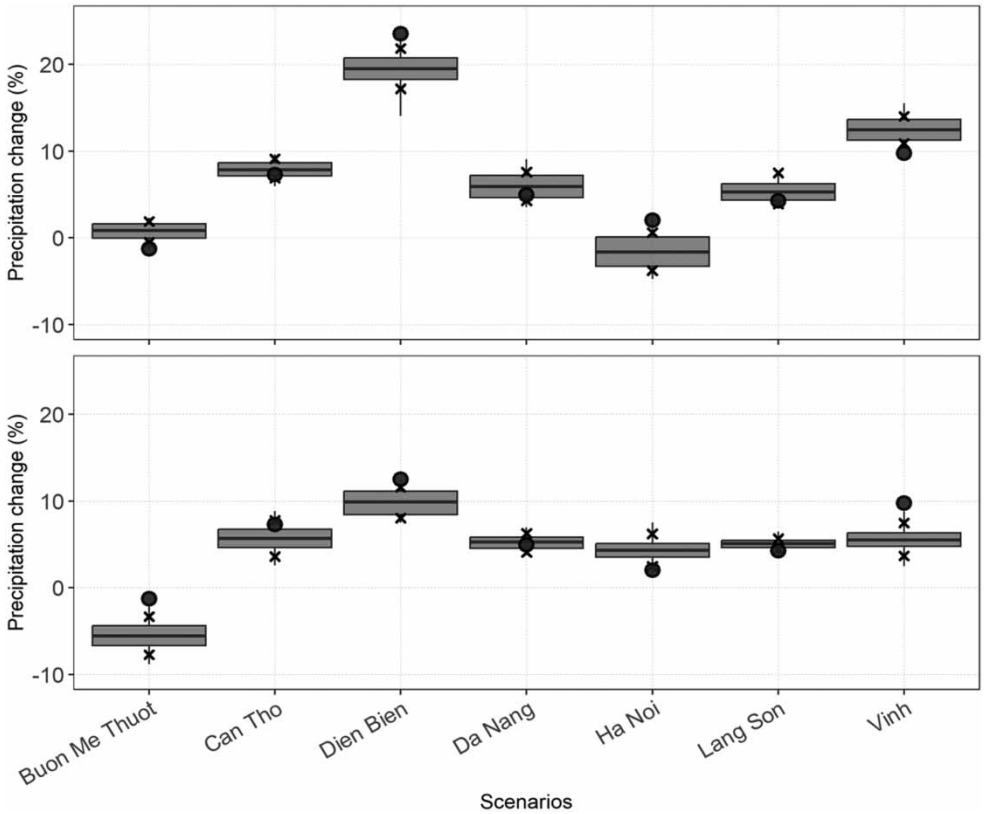

Figure 3 | Same as Figure 2 but for rainfall.

stations range from approximately −5.5% under RCP8.5 (−1.5% under RCP4.5) at the Ban Me Thuot station to approximately 19.5% under RCP4.5 (23% under RCP4.5) at the Dien Bien station, reflecting significant spatial variability in rainfall. For both scenarios, the SMME model members demonstrate consistency among themselves, as indicated by the narrow 5th–95th percentile range for future rainfall estimates, varying from 2.18% at the Can Tho station under RCP4.5 to 7.09% at the Dien Bien station under RCP4.5. Generally, the observed changes fall within the SMME range. It is noteworthy that changes in rainfall at three out of seven stations in both RCP4.5 and RCP8.5 scenarios fall outside the SMME 5th–95th percentile range, highlighting the importance of the SMME ensemble in representing rainfall extreme values that may occur in the tail of the distribution.

Temperature and rainfall projections

Figure 4 presents the projected warming trend of global and Vietnam average temperatures based on the CMIP5 GCMs and CMIP5-VN downscaled experiments. The median of the temperature anomaly between the period 2080–2099 and the baseline period 1986–2005 is projected to increase by 2.06 and 3.78 °C under RCP4.5 and RCP8.5, respectively. In Vietnam, the warming trend is slightly less severe compared to the global scale, with a median temperature anomaly of 1.98 °C (3.56 °C) under RCP4.5 (RCP8.5), as projected by the CMIP5-VN downscaled experiments. This result aligns with previous findings (e.g., Arias *et al.* 2021; Tran-Anh *et al.* 2022) since Vietnam is located in a relatively lower latitude zone, resulting in less ice–albedo feedback compared to colder regions in the high latitude areas. The ensemble average of the SMME models exhibits slightly warmer conditions than those of the CMIP5 GCMs and CMIP5-VN experiments for both global and Vietnam average temperatures, particularly in the far future. The projected temperature for Vietnam displays higher variability compared to the global scale. By the end of the century, the uncertainty range of the CMIP5-VN experiments is larger than that of the CMIP5 GCM ensemble for the global scale. However, the uncertainty range of the SMME models is rather similar for both Vietnam and the global scale. It is also important

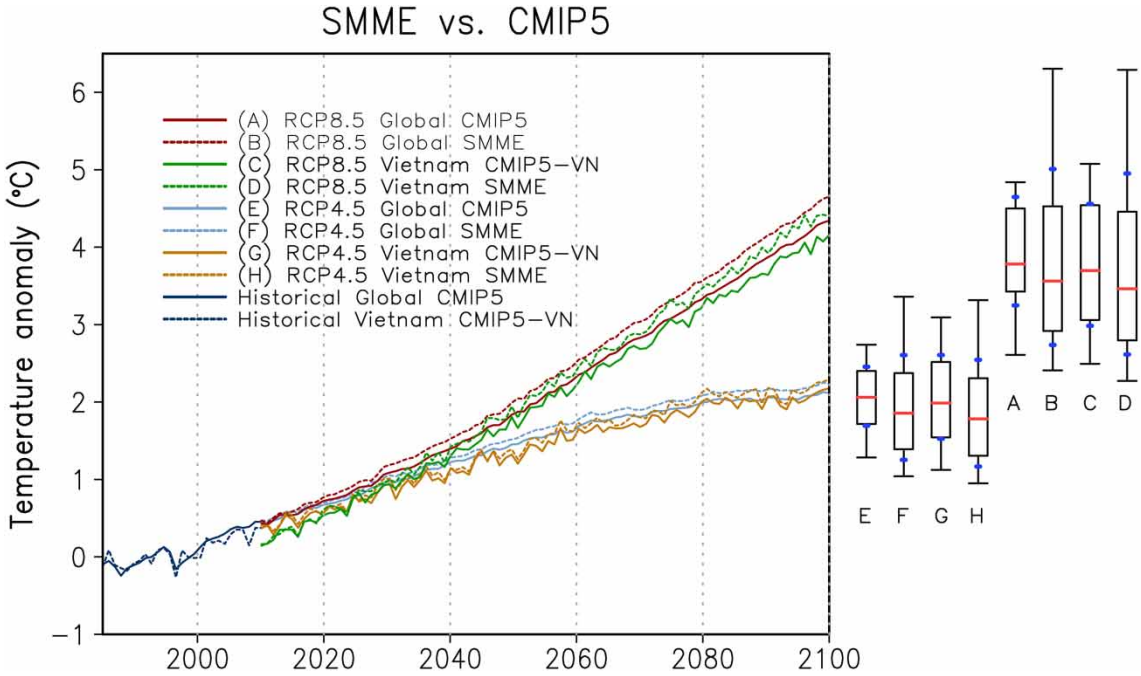

Figure 4 | Temperature anomaly relative to 1986–2005, represented by 5-year moving average lines. Box plots on the right side depict the uncertainty ranges for temperature anomaly projections during 2080–2099, with the box representing the interquartile range, the middle red line indicating the median, and the upper and lower ends of the vertical black lines representing the 95th and 5th quantiles, respectively. In addition, the 83rd and 17th quantiles are indicated by blue dots.

to note that the SMME models well preserve the temperature trends observed in both the CMIP5-VN and CMIP5 GCM ensembles.

The SMME models can capture extreme probability distributions that the CMIP5 models cannot represent. Indeed, the SMME cumulative distribution functions (CDFs) generally display more weight in the tails of the distribution functions (Figure 5(a)–5(d)) for both global and Vietnam temperature averages. Similarly, Figure 5(e)–5(h) demonstrates that the SMME models notably focus more on the extreme tails of changes in rainfall, not only for annual values but also for seasonal averages in both Northern and Southern Vietnam under both RCP4.5 and RCP8.5, compared to the combined CMIP5-VN models. With its larger projection range over the traditional ensemble method, the SMME approach is expected to yield more comprehensive results in studying future extreme climate conditions in Vietnam.

Figure 6 displays the probabilistic projection results of temperature warming under RCP8.5 for Vietnam using the SMME-VN dataset. The trend of increasing temperatures across Vietnam is evident for all percentiles. There is a considerable difference in temperature rise between the 5th (2.27 °C) and 95th percentile (6.29 °C), indicating a large uncertainty range in the projected future outcomes. Moreover, the spatial and temporal distribution of temperature increase differs significantly. Northern Vietnam is projected to experience the highest level of warming in the country (2.46–6.93 °C), whereas moving toward lower latitudes results in lower temperature increases, with Southern Vietnam showing the least warming (2.16–5.82 °C). Regarding seasonal temperature distribution, the average warming in March–April–May (MAM) and September–October–November (SON) surpasses that of June–July–August (JJA) and December–January–February (DJF), with the highest projected in MAM (2.25–6.38 °C) and the lowest in DJF (2.24–6.21 °C).

The SMME-VN also reveals a slight upward trend in average annual rainfall across Vietnam at the end of the 21st century (Figure 7), with an increase of 2.18–6.12% corresponding to the 5th–95th percentile interval. Unlike temperatures, which exhibit significant increases in both space and time, the distribution of increased rainfall occurs only in specific areas and seasons. Notably, annual rainfall is projected to increase most significantly in the South-Central Coast (5.7–14.2%, corresponding to the 5–95th percentile), followed by the North-Central Coast (4.54–10.18%), the Central Highlands (2.77–7.51%), and the northern mountains in Northwest Vietnam (0.13–3.85%). Meanwhile, the southern region shows no obvious change in annual rainfall. As for seasonal rainfall distribution, the increasing trend is prominent across Vietnam during JJA,

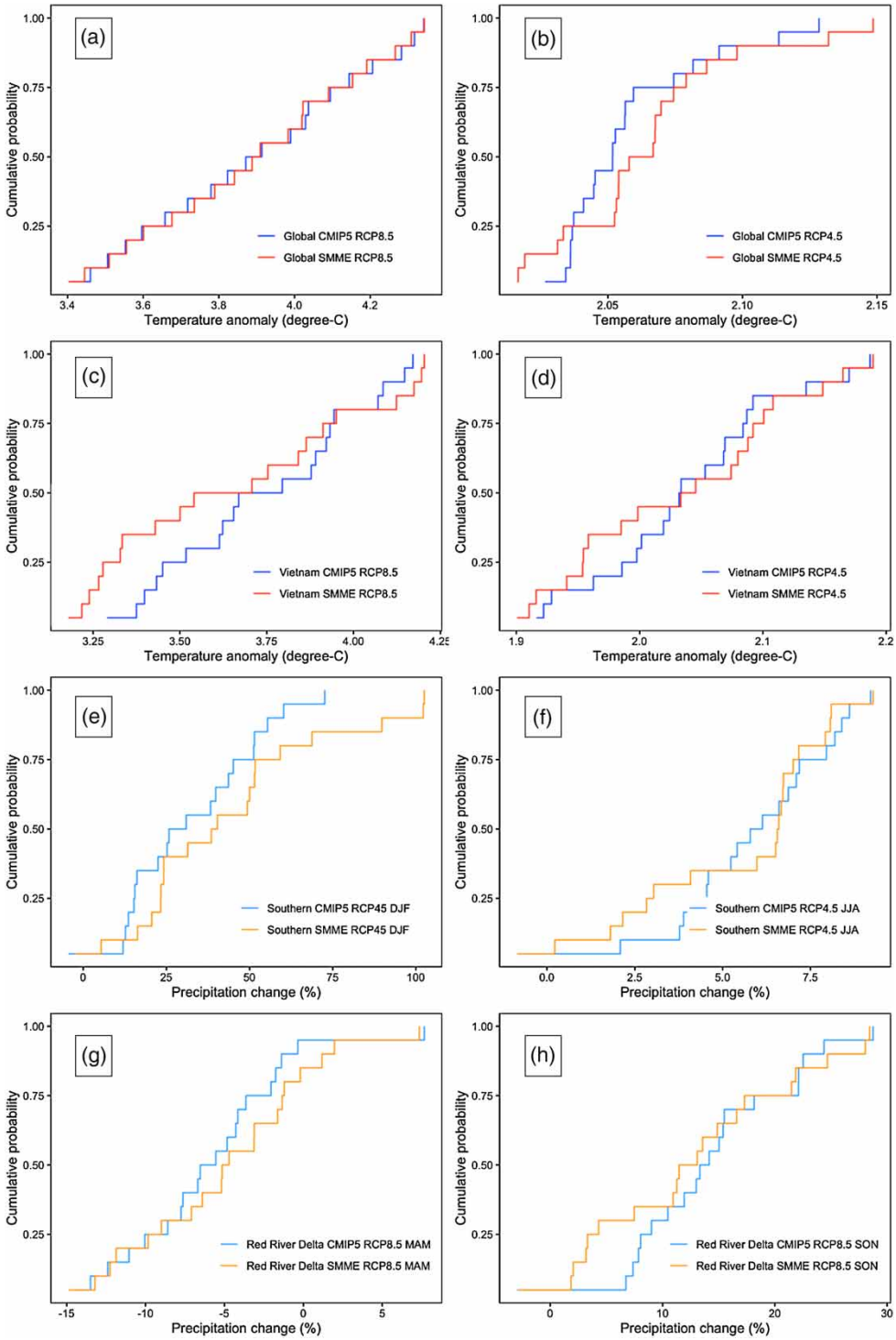

Figure 5 | CDFs of temperature and rainfall anomalies for the period 2080–2099 relative to the 1986–2005 norms. (a) and (b) display CDFs of global temperature averages, while (c) and (d) show results for Vietnam. (e) and (f) depict CDFs of DJF and JJA seasonal rainfall over southern Vietnam, respectively. (g) and (h) illustrate CDFs of MAM and SON seasonal rainfall over the Red River Delta in northern Vietnam. Each panel presents results from both SMME models and CMIP5 GCMs (CMIP5-VN).

followed by SON. During MAM, there is no clear trend in rainfall. Regarding DJF, the South-Central Coast region is projected to experience a remarkable increasing trend in rainfall. In brief, more extreme rainfall is projected to occur in the future, particularly over the central regions of Vietnam.

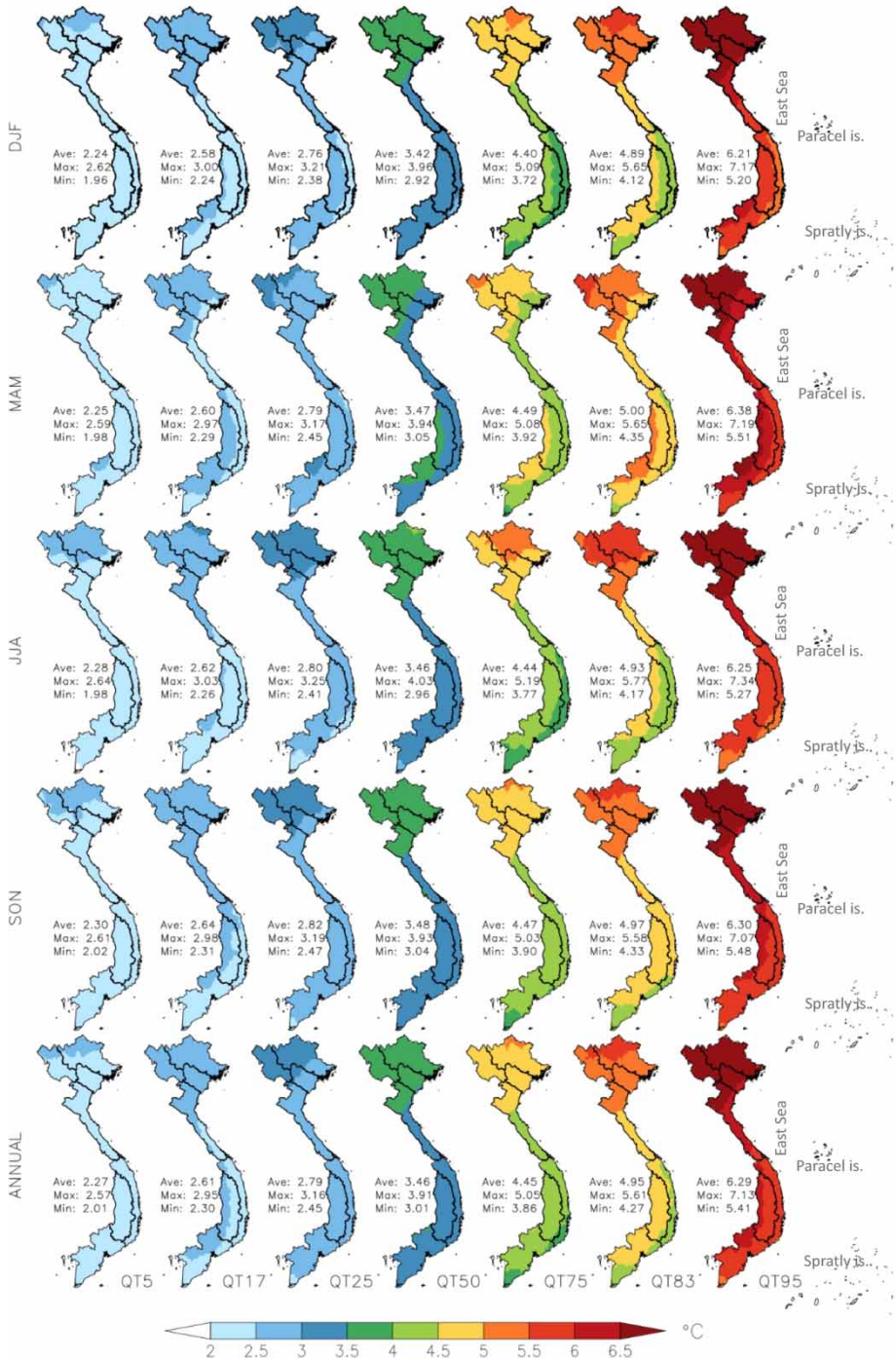

Figure 6 | Projected changes in seasonal and annual temperature for the period 2080–2099 under RCP8.5, relative to the baseline period. The SMME-VN results for quantiles ranging from the 5th to the 95th percentile are shown from left to right.

Uncertainty sources of the projections' results

The proportion of uncertainty sources in the CMIP5 GCMs and SMME models for projecting temperature increases at the global scale and in four major cities in Vietnam is depicted in Figure 8. These cities include Hanoi and Quang Ninh in the north, Da Nang in the central region, and Ho Chi Minh in southern Vietnam. At the beginning of the 21st century, unforced uncertainty dominates the total model uncertainty. However, it rapidly diminishes over time as uncertainty from the

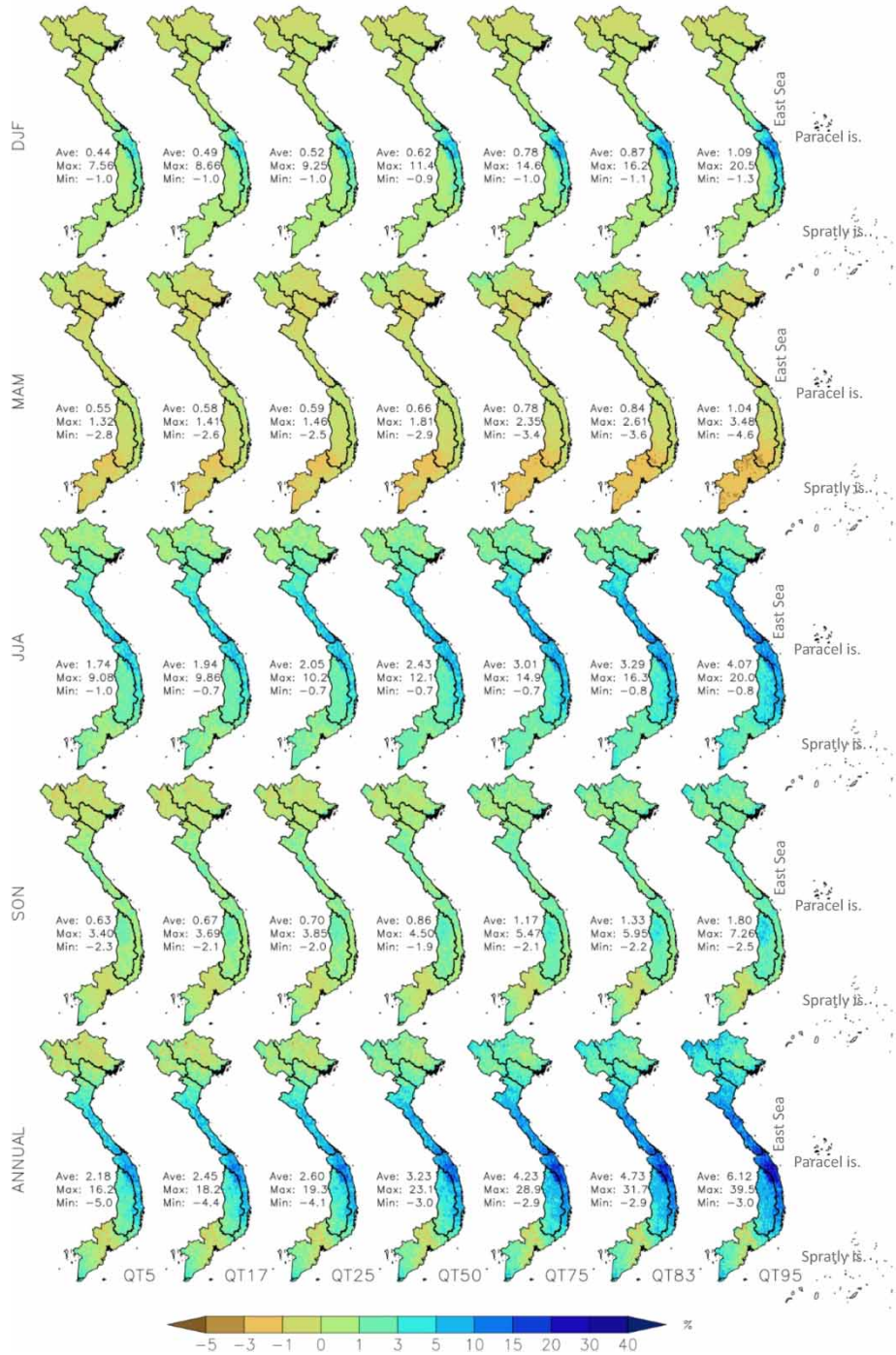

Figure 7 | Same as Figure 6 but for rainfall.

scenarios and forced climate change increases, especially from the RCP scenarios. By the end of the century, unforced climate change uncertainty nearly disappears, and the primary contributor to total uncertainty becomes scenario uncertainty, accounting for approximately 75–80% of the total signal. Forced uncertainty, although tending to increase over time, remains relatively moderate, reaching a maximum of 20–25% in the period 2080–2099. In the four major cities of Vietnam, the changing trend of climate change uncertainty sources is expected to be similar to that at the global scale, but the trend of increasing uncertainty from the two RCP scenarios is lower. Notably, the proportion of scenario uncertainty (forced uncertainty) in the

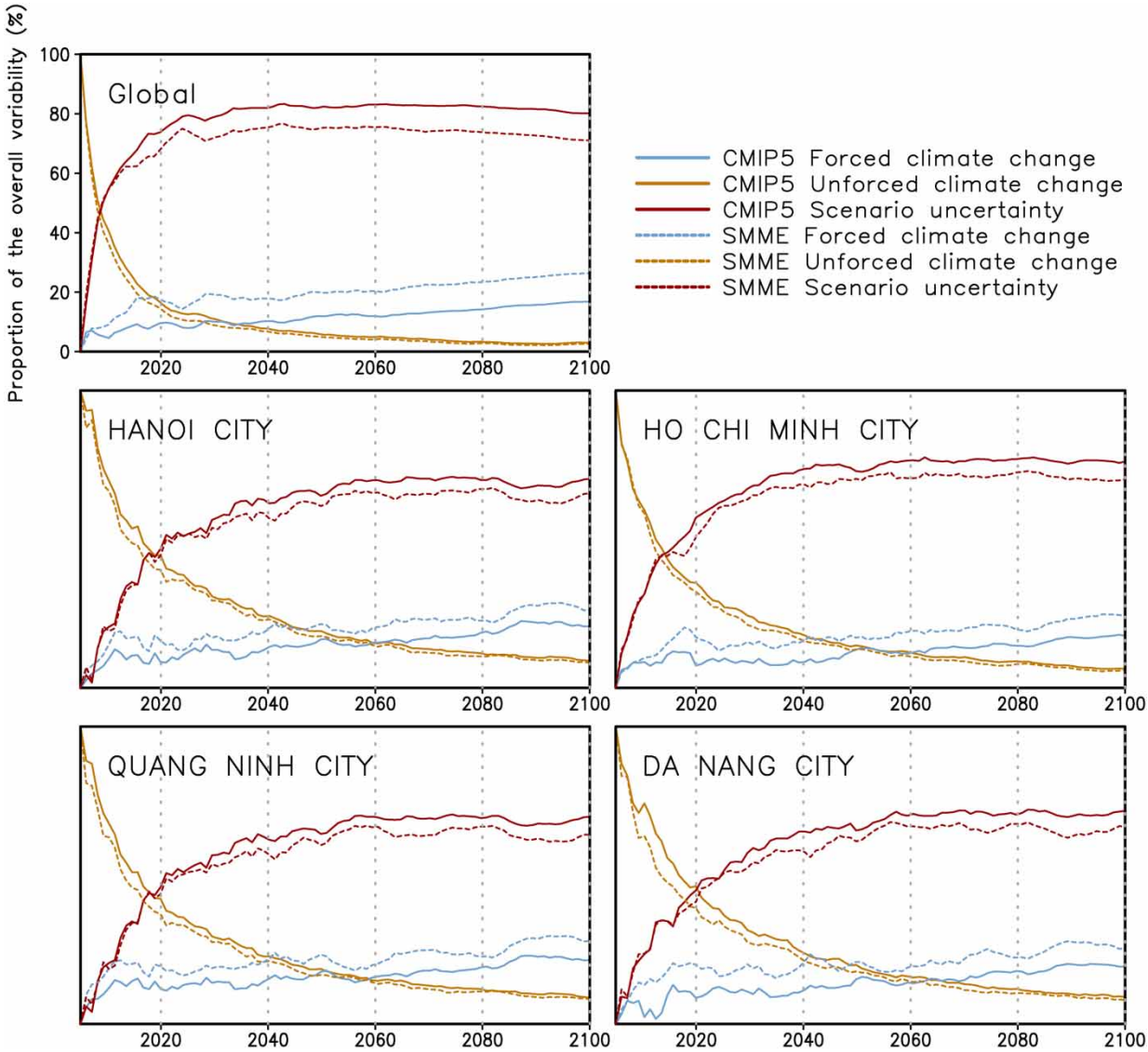

Figure 8 | Ratio of temperature anomaly projection uncertainty sources in the simulation outputs of two model ensembles, the CMIP5 GCMs (CMIP5-VN) (solid line) and the SMME models (dashed line). The red, blue, and yellow lines represent the uncertainty values of forced climate change, unforced climate change, and uncertainty between scenarios, respectively, for (a) the global scale, (b) Hanoi, (c) Ho Chi Minh, (d) Quang Ninh, and (e) Da Nang.

SMME models is smaller (higher) than that in the CMIP5 GCMs for the future period. Meanwhile, unforced uncertainty remains quite consistent over time between the two sets of models.

CONCLUSIONS

This study has successfully developed the SMME-VN dataset for future probabilistic projections of climate change in Vietnam, with a specific focus on temperature and rainfall. The dataset was constructed using the SMME method and the outputs of 31 CMIP5 GCMs. Each GCM was assigned a probability weight based on its estimated global temperature anomaly relative to the MAGICC6 temperature probability distribution. Furthermore, SMs were established to capture temperature probabilities in the extreme tails that were not accurately represented by the GCMs. The pattern scaling method was then applied to build the probabilistic model for Vietnam, i.e., the SMME-VN dataset, based on the probability of climate change on a global scale, corresponding to the 5th, 17th, 25th, 50th, 75th, 83rd, and 95th percentiles.

The SMME models demonstrate satisfactory performance in representing temperature and rainfall changes for the period 2006–2018, under both scenarios RCP4.5 and RCP8.5, when compared to the baseline period 1986–2005. Across the seven randomly selected stations, the observed changes generally fall within the SMME ranges. However, it is noticeable that changes in rainfall at three out of the seven stations, under both RCP4.5 and RCP8.5 scenarios, fall outside the SMME 5th–95th percentile range. This highlights the importance of the SMME ensemble's ability to represent extreme values that may occur in the tail of the distribution.

The projected SMME temperature for Vietnam, with a 5% probability of occurrence (corresponding to the 95th percentile), exhibits an increase of 5.41–7.13 °C during the period 2080–2099 under the RCP8.5 scenario compared to the baseline period 1986–2005. The northern region is projected to experience more warming compared to the central and southern regions. SMME-VN projects a slight increase in average rainfall across the country, with the largest increase occurring in the central region, reaching a maximum of 14.2% at the 95th percentile. Regarding the sources of uncertainty in future projections, unforced uncertainty dominates the total signal during the early part of the 21st century. Forced uncertainty remains relatively moderate but increases gradually over time, reaching a maximum of 20–25% by the period 2080–2099. As we approach the end of the century, the proportion of unforced uncertainty decreases, giving way to uncertainty associated with greenhouse gas scenarios, which accounts for 75–80% of the total signal.

The SMME-VN dataset is accessible online and offers significant potential for diverse applications. We highly recommend employing this dataset for further studies, specifically in quantitatively assessing climate change risks and their impacts on socioeconomic activities in Vietnam. By benefiting from the high-resolution and probabilistic nature of the dataset, policymakers, researchers, and other users can gain valuable insights into a wide range of potential climate outcomes. This, in turn, facilitates more informed decision-making and effective addressing of the challenges posed by future climate change in Vietnam.

AUTHORS CONTRIBUTIONS

QT-A processed data and performed the analysis. Both TN-D and QT-A discussed the results and wrote the manuscript.

FUNDING

This study was supported by the Vietnam National Foundation for Science and Technology Development (NAFOSTED) under Grant 105.06-2021.14. QT-A was supported by the GEMMES project funded by the French Development Agency.

DATA AVAILABILITY STATEMENT

All relevant data are available from an online repository or repositories: https://remosat.usth.edu.vn/Download/dat_GEMMES_WP1/SMME_CMIP5/.

CONFLICT OF INTEREST

The authors declare there is no conflict.

REFERENCES

Arias, P. A., Bellouin, N., Coppola, E., Jones, R. G., Krinner, G., Marotzke, J., Naik, V., Palmer, M. D., Plattner, G. K., Rogelj, J., Rojas, M., Sillmann, J., Storelvmo, T., Thorne, P. W., Trewin, B., Achuta Rao, K., Adhikary, B., Allan, R. P., Armour, K., Bala, G., Barimalala, R., Berger, S., Canadell, J. G., Cassou, C., Cherchi, A., Collins, W., Collins, W. D., Connors, S. L., Corti, S., Cruz, F., Dentener, F. J., Dereczynski, C., di Luca, A., Diongue Niang, A., Doblas-Reyes, F. J., Dosio, A., Douville, H., Engelbrecht, F., Eyring, V., Fischer, E., Forster, P., Fox- Kemper, B., Fuglestvedt, J. S., Fyfe, J. C., Gillett, N. P., Goldfarb, L., Gorodetskaya, I., Gutierrez, J. M., Hamdi, R., Hawkins, E., Hewitt, H. T., Hope, P., Islam, A. S., Jones, C., Kaufman, D. S., Kopp, R. E., Kosaka, Y., Kossin, J., Krakovska, S., Lee, J. Y., Li, J., Mauritsen, T., Maycock, T. K., Meinshausen, M., Min, S. K., Monteiro, P. M. S., Ngo-Duc, T., Otto, F., Pinto, I., Pirani, A., Raghavan, K., Ranasinghe, R., Ruane, A. C., Ruiz, L., Sallée, J. B., Samset, B. H., Sathyendranath, S., Seneviratne, S. I., Sörensson, A. A., Szopa, S., Takayabu, I., Tréguier, A. M., van den Hurk, B., Vautard, R., von Schuckmann, K., Zaehle, S., Zhang, X., Zickfeld, K, . 2021 Technical summary. In: *Climate Change 2021: The Physical Science Basis. Contribution of Working Group I to the Sixth Assessment Report of the Intergovernmental Panel on Climate Change* (Masson-Delmotte, V., Zhai, P., Pirani, A., Connors, S. L., Péan, C., Berger, S., Caud, N., Chen, Y., Goldfarb, L., Gomis, M. I., Huang, M., Leitzell, K., Lonnoy, E., Matthews, J. B. R., Maycock, T. K., Waterfield, T., Yelekçi, O., Yu, R. & Zhou, B., eds). Cambridge University Press, Cambridge, UK, pp. 33–144. https://doi.org/10.1017/9781009157896.002.

Atiah, W. A., Johnson, R., Muthoni, F. K., Mengistu, G. T., Amekudzi, L. K., Kwabena, O. & Kizito, F. 2023 Bias correction and spatial disaggregation of satellite-based data for the detection of rainfall seasonality indices. *Heliyon* **9** (7), e17604. https://doi.org/10.1016/j.heliyon.2023.e17604.

Chen, X., Raftery, A. E., Battisti, D. S. & Liu, P. R. 2023 Long-term probabilistic temperature projections for all locations. *Climate Dynamics* **60** (7), 2303–2314. https://doi.org/10.1007/s00382-022-06441-8.

Collins, M., Knutti, R., Arblaster, J., Dufresne, J.-L., Fichefet, T., Friedlingstein, P., Gao, X., Gutowski, W. J., Johns, T., Krinner, G., Shongwe, M., Tebaldi, C., Weaver, A. J., Wehner, M., 2013 Long-term climate change: Projections, commitments and irreversibility. In: *Climate Change 2013: The Physical Science Basis. Contribution of Working Group I to the Fifth Assessment Report of the Intergovernmental Panel on Climate Change* (Stocker, T. F., Qin, D., Plattner, G.-K., Tignor, M., Allen, S. K., Boschung, J., Nauels, A., Xia, Y., Bex, V. & Midgley, P. M., eds.). Cambridge University Press, Cambridge, UK, pp. 1029–1136.

Dasgupta, S., Laplante, B., Meisner, C., Wheeler, D. & Yan, J. 2007 *The Impact of Sea Level Rise on Developing Countries: A Comparative Analysis*. The World Bank, Washington, DC, p. 51. Available from: http://hdl.handle.net/10986/7174.

David, E., Vera, K. & Laura, S. 2018 *Global Climate Risk Index 2018: Who Suffers Most From Extreme Weather Events? Weather-Related Loss Events in 2016 and 1997 to 2016*. Germanwatch e.V, p. 36. Available from: https://www.germanwatch.org/en/cri.

de Elía, R., Biner, S. & Frigon, A. 2013 Interannual variability and expected regional climate change over North America. *Climate Dynamics* **41**, 1245–1267. https://doi.org/10.1007/s00382-013-1717-9.

Deser, C., Phillips, A., Bourdette, V. & Teng, H. 2012 Uncertainty in climate change projections: The role of internal variability. *Climate Dynamics* **38** (3–4), 527–546. https://doi.org/10.1007/s00382-010-0977-x.

Duan, C., Wang, P., Cao, W., Wang, X., Wu, R. & Cheng, Z. 2021 Improving the spring air temperature forecast skills of bcc_csm1. 1(M) by spatial disaggregation and bias correction: Importance of trend correction. *Atmosphere* **12** (9), 1143. https://doi.org/10.3390/atmos12091143.

Espagne, E., Ngo-Duc, T., Nguyen, M.-H., Pannier, E., Woillez, M.-N., Drogoul, A., Huynh, T. P. L., Le, T. T., Nguyen, T. T. H., Nguyen, T. T., Nguyen, T. A., Thomas, F., Truong, C. Q., Vo, Q. T. & Vu, C. T. 2021 *Climate Change in Viet Nam: Impacts and Adaptation. A COP26 Assessment Report of the GEMMES Viet Nam Project*. Agence Française de Développement, Paris, p. 612. Available from: https://www.afd.fr/en/ressources/climate-change-viet-nam-impacts-and-adaptation.

Gergel, D. R., Malevich, S. B., McCusker, K. E., Tenezakis, E., Delgado, M. T., Fish, M. A. & Kopp, R. E. 2024 Global downscaled projections for climate impacts research (GDPCIR): Preserving quantile trends for modeling future climate impacts. *Geoscientific Model Development***17**, 191–227. https://doi.org/10.5194/gmd-17-191-2024.

Hawkins, E. & Sutton, R. 2009 The potential to narrow uncertainty in regional climate predictions. *Bulletin of the American Meteorological Society* **90** (8), 1095–1108. https://doi.org/10.1175/2009BAMS2607.1.

Herrmann, M., Nguyen-Duy, T., Ngo-Duc, T. & Tangang, F. 2022 Climate change impact on sea surface winds in Southeast Asia. *International Journal of Climatology* **42** (7), 3571–3595. https://doi.org/10.1002/joc.7433.

Houser, T., Hsiang, S., Kopp, R., Larsen, K., Delgado, M., Jina, A., Mastrandrea, M., Mohan, S., Muir-Wood, R., Rasmussen, D. J., Rising, J., Wilson, P., Fisher-Vanden, K., Greenstone, M., Heal, G., Oppenheimer, M., Stern, N., Ward, B. & Paulson, H. M. 2015 *Economic Risks of Climate Change: An American Prospectus*. Columbia University Press, p. 384. https://doi.org/10.7312/hous17456.

Iles, C. E., Vautard, R., Strachan, J., Joussaume, S., Eggen, B. R. & Hewitt, C. D. 2020 The benefits of increasing resolution in global and regional climate simulations for European climate extremes. *Geoscientific Model Development*. 13 (11), 5583–5607. https://doi.org/10.5194/gmd-13-5583-2020.

Karl, T. R., Nicholls, N. & Ghazi, A. 1999 CLIVAR/GCOS/WMO workshop on indices and indicators for climate extremes: Workshop summary. *Climatic Change* **42**, 3–7.

Katzfey, J., Nguyen, K., McGregor, J., Hoffmann, P., Ramasamy, S., Nguyen, H. V., Khiem, M. V., Nguyen, T. V., Truong, K. B., Vu, T. V., Nguyen, H. T., Thuc, T., Phong, D. H., Nguyen, B. T., Phan-Van, T., Nguyen-Quang, T., Ngo-Duc, T. & Trinh-Tuan, L. 2016 High-resolution simulations for Vietnam – Methodology and evaluation of current climate. *Asia-Pacific Journal of Atmospheric Sciences* **52** (2), 91–106. https://doi.org/10.1007/s13143-016-0011-2.

Kitoh, A. & Endo, H. 2016 Changes in precipitation extremes projected by a 20-km mesh global atmospheric model. *Weather and Climate Extremes* **11**, 41–52. https://doi.org/10.1016/j.wace.2015.09.001.

Kopp, R. & Rasmussen, D. J. 2015 Appendix A. Physical climate projections. In: *Economic Risks of Climate Change: An American Prospectus.* New York Chichester, West Sussex: Columbia University Press, pp. 219–248. https://doi.org/10.7312/hous17456-029.

Lehner, B., Verdin, K. & Jarvis, A. 2008 New global hydrography derived from spaceborne elevation data. *Eos, Transactions, American Geophysical Union* **89** (10), 93–94. https://doi.org/10.1029/2008eo100001.

Liu, P. R. & Raftery, A. E. 2021 Country-based rate of emissions reductions should increase by 80% beyond nationally determined contributions to meet the 2°C target. *Communications Earth & Environment* **2**, 29. https://doi.org/10.1038/s43247-021-00097-8.

Luo, Y., Zhang, R., Wang, H. & Lu, J. 2019 Combining multiple GCMs for improved seasonal ensemble precipitation forecast for the Huai River basin, China. *Climate Dynamics* **53** (5), 2999–3014.

Maurer, E. P. & Hidalgo, H. G. 2008 Utility of daily vs. monthly large-scale climate data: An intercomparison of two statistical downscaling methods. *Hydrology and Earth System Sciences* **12**, 551–563. https://doi.org/10.5194/hess-12-551-2008.

Meinshausen, M., Raper, S. C. B. & Wigley, T. M. L. 2011 Emulating coupled atmosphere-ocean and carbon cycle models with a simpler model, MAGICC6 – Part 1: Model description and calibration. *Atmospheric Chemistry and Physics* **11** (4), 1417–1456. https://doi.org/10.5194/acp-11-1417-2011.

Michalek, A. T., Villarini, G. & Kim, T. 2024 Understanding the impact of precipitation bias-correction and statistical downscaling methods on projected changes in flood extremes. *Earth's Future* **12** (3), e2023EF004179. https://doi.org/10.1029/2023EF004179.

MONRE. 2009 *Climate Changes and Sea Level Rise Scenarios for Viet Nam*. Ministry of Natural Resources and Environment, Hanoi, p. 34 (in Vietnamese).

MONRE. 2012 *Climate Change, Sea Level Rise Scenarios for Viet Nam*. Ministry of Natural Resources and Environment – Viet Nam Natural Resources, Environment and Mapping Publishing House, Hanoi, p. 112 (in Vietnamese).

MONRE. 2016 *Climate Change, Sea Level Rise Scenarios for Viet Nam*. Ministry of Natural Resources and Environment – Viet Nam Natural Resources, Environment and Mapping Publishing House, Hanoi, p. 188 (in Vietnamese).

MONRE. 2020 *Climate Change, Sea Level Rise Scenarios for Viet Nam*. Ministry of Natural Resources and Environment – Viet Nam Natural Resources, Environment and Mapping Publishing House, Hanoi, p. 286 (in Vietnamese).

Moss, R. H., Edmonds, J. A., Hibbard, K. A., Manning, M. R., Rose, S. K., Van Vuuren, D. P., Carter, T. R., Emori, S., Kainuma, M., Kram, T., Meehl, G. A., Mitchell, J. F. B., Nakicenovic, N., Riahi, K., Smith, S. J., Stouffer, R. J., Thomson, A. M., Weyant, J. P. & Wilbanks, T. J. 2010 The next generation of scenarios for climate change research and assessment. *Nature* **463** (7282), 747–756. https://doi.org/10.1038/nature08823.

Ngo-Duc, T., Kieu, C., Thatcher, M., Nguyen-Le, D. & Phan-Van, T. 2014 Climate projections for Vietnam based on regional climate models. *Climate Research* **60** (3), 199–213. https://doi.org/10.3354/cr01234.

Nguyen, D. N. & Nguyen, T. H. 2004 *Vietnamese Climate and Climatic Resources*. Science and Technology Publishing House, Vietnam, p. 230 (in Vietnamese).

Nguyen-Duy, T., Ngo-Duc, T. & Desmet, Q. 2023 Performance evaluation and ranking of CMIP6 global climate models over Vietnam. *Journal of Water and Climate Change* **14** (6), 1831. https://doi.org/10.2166/wcc.2023.454.

Nguyen-Thuy, H., Ngo-Duc, T., Trinh-Tuan, L., Tangang, F., Cruz, F., Phan-Van, T., Juneng, L., Narisma, G. & Santisirisomboon, J. 2021 Time of emergence of climate signals over Vietnam detected from the CORDEX-SEA experiments. *International Journal of Climatology* **41** (3), 1599–1618. https://doi.org/10.1002/joc.6897.

Nishant, N., Di Virgilio, G., Ji, F., Tam, E., Beyer, K. & Riley, M. L. 2022 Evaluation of present-day CMIP6 model simulations of extreme precipitation and temperature over the Australian continent. *Atmosphere* **13** (9), 1478. https://doi.org/10.3390/atmos13091478.

Rabezanahary Tanteliniaina, M. F. & Andrianarimanana, M. H. 2024 Projection of future drought characteristics in the Great South of Madagascar using CMIP6 and bias-correction spatial disaggregation method. *Theoretical and Applied Climatology* **155** (3), 1871–1883. https://doi.org/10.1007/s00704-023-04727-3.

Raftery, A. E., Zimmer, A., Frierson, D. M. W., Startz, R. & Liu, P. 2017 Less than 2°C warming by 2100 unlikely. *Nature Climate Change* **7** (9), 637–641. https://doi.org/10.1038/nclimate3352.

Rasmussen, D. J., Meinshausen, M. & Kopp, R. E. 2016 Probability-weighted ensembles of U. S. county-level climate projections for climate risk analysis. *Journal of Applied Meteorology and Climatology* **55** (10), 2301–2322. https://doi.org/10.1175/JAMC-D-15-0302.1.

Santer, B. D., Wigley, T. M. L., Schlesinger, M. E. & Mitchell, J. F. B. 1990 *Developing Climate Scenarios From Equilibrium GCM Results*. Max-Planck-Institut für Meteorologie Rep. 47, p. 29 Available from: https://www.mpimet.mpg.de/fileadmin/publikationen/Reports/Report_47.pdf.

Schölzel, C. & Hense, A. 2011 Probabilistic assessment of regional climate change in Southwest Germany by ensemble dressing. *Climate Dynamics* **36** (9–10), 2003–2014. https://doi.org/10.1007/s00382-010-0815-1.

Seneviratne, S. I., Nicholls, N., Easterling, D., Goodess, C. M., Kanae, S., Kossin, J., Luo, Y., Marengo, J., McInnes, K., Rahimi, M., Reichstein, M., Sorteberg, A., Vera, C., Zhang, X., 2012 Changes in climate extremes and their impacts on the natural physical environment. In: *Managing the Risks of Extreme Events and Disasters to Advance Climate Change Adaptation* (Field, C. B., Barros, V., Stocker, T. F., Qin, D., Dokken, D. J., Ebi, K. L., Mastrandrea, M. D., Mach, K. J., Plattner, G.-K., Allen, S. K., Tignor, M. & Midgley, P. M., eds). A Special Report of Working Groups I and II of the Intergovernmental Panel on Climate Change (IPCC). Cambridge University Press, Cambridge, UK, pp. 109–230.

Sorteberg, A. & Kvamstø, N. G. 2006 The effect of internal variability on anthropogenic climate projections. *Tellus A* **58** (5), 565–574. https://doi.org/10.1111/j.1600-0870.2006.00202.x.

Supari, S., Tangang, F., Juneng, L., Cruz, F., Chung, J. X., Ngai, S. T., Salimun, E., Mohd, M. S. F., Santisirisomboon, J., Singhruck, P., Tan, P. V., Ngo-Duc, T., Narisma, G., Aldrian, E., Gunawan, D. & Sopaheluwakan, A. 2020 Multi-model projections of precipitation extremes in Southeast Asia based on CORDEX-Southeast Asia simulations. *Environmental Research* **184**, 109350. https://doi.org/10.1016/j.envres.2020.109350.

Switzer, P., 2014 Kriging. In: *Wiley StatsRef: Statistics Reference Online* (Balakrishnan, N., Colton, T., Everitt, B., Piegorsch, W., Ruggeri, F. & Teugels, J. L., eds). Wiley. https://doi.org/10.1002/9781118445112.stat03708.

Tangang, F., Chung, J. X., Juneng, L., Supari, Salimun, E., Ngai, S. T., Jamaluddin, A. F., Mohd, M. S. F., Cruz, F., Narisma, G., Santisirisomboon, J., Ngo-Duc, T., Tan, P. V., Singhruck, P., Gunawan, D., Aldrian, E., Sopaheluwakan, A., Grigory, N., Remedio, A. R. C., Sein, D. V., Hein-Griggs, D., McGregor, J. L., Yang, H., Sasaki, H. & Kumar, P. 2020 Projected future changes in rainfall in Southeast Asia based on CORDEX–SEA multi-model simulations. *Climate Dynamics* **55** (5), 1247–1267. https://doi.org/10.1007/s00382-020-05322-2.

Taylor, K. E., Stouffer, R. J. & Meehl, G. A. 2012 An overview of CMIP5 and the experiment design. *Bulletin of the American Meteorological Society* **93** (4), 485–498. https://doi.org/10.1175/BAMS-D-11-00094.1.

Tebaldi, C. & Arblaster, J. M. 2014 Pattern scaling: Its strengths and limitations, and an update on the latest model simulations. *Climatic Change* **122** (3), 459–471. https://doi.org/10.1007/s10584-013-1032-9.

Tebaldi, C., Smith, R. L., Nychka, D. & Mearns, L. O. 2005 Quantifying uncertainty in projections of regional climate change: A Bayesian approach to the analysis of multimodel ensembles. *Journal of Climate* **18** (10), 1524–1540.

Tran-Anh, Q., Ngo-Duc, T., Espagne, E. & Trinh-Tuan, L. 2022 A high-resolution projected climate dataset for Vietnam: Construction and preliminary application in assessing future change. *Journal of Water and Climate Change* **13** (9), 3379–3399. https://doi.org/10.2166/wcc.2022.144.

Tran-Anh, Q., Ngo-Duc, T., Espagne, E. & Trinh-Tuan, L. 2023 A 10-km CMIP6 downscaled dataset of temperature and precipitation for historical and future Vietnam climate. *Scientific Data* **10** (1), 257. https://doi.org/10.1038/s41597-023-02159-2.

Trinh-Tuan, L., Matsumoto, J., Tangang, F. T., Juneng, L., Cruz, F., Narisma, G., Santisirisomboon, J., Phan-Van, T., Gunawan, D., Aldrian, E. & Ngo-Duc, T. 2019 Application of quantile mapping bias correction for mid-future precipitation projections over Vietnam. *Scientific Online Letters on the Atmosphere* **15**, 1–6. https://doi.org/10.2151/SOLA.2019-001.

Vargas Zeppetello, L. R., Raftery, A. E. & Battisti, D. S. 2022 Probabilistic projections of increased heat stress driven by climate change. *Communications Earth & Environment* **3**, 183. https://doi.org/10.1038/s43247-022-00524-4.

Willmott, C. J., Rowe, C. M. & Philpot, W. D. 1985 Small-scale climate maps: A sensitivity analysis of some common assumptions associated with grid-point interpolation and contouring. *The American Cartographer* **12** (1), 5–16. https://doi.org/10.1559/152304085783914686.

Wood, A. W., Maurer, E. P., Kumar, A. & Lettenmaier, D. 2002 Long-range experimental hydrologic forecasting for the eastern United States. *Journal of Geophysical Research: Atmospheres* **107** (D20), 4429. https://doi.org/10.1029/2001JD000659.

Wood, A. W., Leung, L. R., Sridhar, V. & Lettenmaier, D. P. 2004 Hydrologic implications of dynamical and statistical approaches to downscaling climate model outputs. *Climatic Change* **62** (1–3), 189–216. https://doi.org/10.1023/B:CLIM.0000013685.99609.9e.

World Bank 2022 *Vietnam Country Climate and Development Report. CCDR Series*. Washington, DC, p. 88. Available from: http://hdl.handle.net/10986/37618.

Xin, X., Zhang, L., Zhang, J., Wu, T. & Fang, Y. 2013 Climate change projections over East Asia with BCC_CSM1.1 climate model under RCP scenarios. *Journal of the Meteorological Society of Japan* **91** (4), 413–429. https://doi.org/10.2151/jmsj.2013-401.

Yang, Y., Tang, J., Xiong, Z., Wang, S. & Yuan, J. 2019 An intercomparison of multiple statistical downscaling methods for daily precipitation and temperature over China: Present climate evaluations. *Climate Dynamics* **53** (7–8), 4629–4649. https://doi.org/10.1007/s00382-019-04809-x.

Zhang, S., Chen, F., He, X. & Liu, B. 2017 A new downscaling approach and its performance with bias correction and spatial disaggregation as contrast. *Journal of Water and Climate Change* **8** (4), 675–690. https://doi.org/10.2166/wcc.2017.010.

First received 16 August 2023; accepted in revised form 10 April 2024. Available online 22 April 2024